Two-Component Signaling System RegAB Represses *Pseudomonas syringae* pv. *actinidiae* T3SS by Directly Binding to the promoter of *hrpRS*[1]

Mengsi Zhang[1, 2*], Mingming Yang[2, 3*], Xiaoxue Zhang[1, 2], Shuying Li[1, 2], Shuaiwu Wang[1, 2], Alex Muremi Fulano[4], Yongting Meng[1, 2], Xihui Shen[1, 2], Li-li Huang[2, 3#], Yao Wang[1, 2#]

[1] *College of Life Sciences, Northwest A&F University, Yangling 712100, China.*

[2] *State Key Laboratory for Crop Stress Resistance and High-Efficiency Production, Northwest A&F University, Yangling 712100, China.*

[3] *College of Plant Protection, Northwest A&F University, Yangling 712100, China.*

[4] *Department of Plant Science and Crop Protection, University of Nairobi, Nairobi, Kenya*

Abstract: Kiwifruit bacterial canker, caused by *Pseudomonas syringae* pv. *actinidiae* (*Psa*), is a significant threat to the kiwifruit industry. The two-component signaling systems (TCSs) play a crucial role in regulating the virulence of *Pseudomonas syringae* (*P. syringae*), yet their specific function in *Psa* remains largely unclear. In this study, we found that disrupting the TCS RegAB (encoded by *Psa*_802/*Psa*_803) resulted in a notable increase in the pathogenicity of *Pseudomonas syringae* pv. *actinidiae* M228 (*Psa* M228) in host plant and hypersensitive reaction (HR) in nonhost plant. Through comparative transcriptome analysis of the *Psa* M228 wild-type strain and the *regA* mutant, we identified the pivotal role of RegA/B in controlling various physiological pathways, including the Type III secretion system (T3SS), a key determinant of *Psa* virulence. Additionally, we discovered that the RegA does have binding sites in the promoter region of the *hrpR*/*S*, and the transcriptional level of the *hrpR* and other T3SS-related genes increased in the *regA* deletion strain relative to the *Psa* M228 wild-type. The DNA-binding affinity of RegA, and therefore the repressor function, is enhanced by its phosphorylation. Our findings unveil the function of TCS RegAB and the regulatory mechanism of T3SS by RegAB in *Psa*, highlighting the diverse functions of the RegAB system.

Keywords: *Pseudomonas syringae* pv. *actinidiae*, Type III secretion system (T3SS), Two-component signaling system RegAB, *hrpR*/*S*

1. Introduction

Kiwifruit (*Actinidia* spp.) is plagued by various pathogens, impacting its economic importance. *Pseudomonas syringae* pv. *actinidiae* (*Psa*), the etiological agent of bacterial canker, is one of the most

[1] Mengsi Zhang, Tel: +86-18838964968, E-mail: 188838964968@163.com; Mingming Yang, Tel: +86-13260828693, E-mail: yangming862@126.com; [#]Correspondence Yao Wang, Tel: +86-13488215263, E-mail: wangyao@nwafu.edu.cn; Lili Huang, Tel: +86-13991351090, E-mail: huanglili@nwsuaf.edu.cn

* equal contribution.

destructive diseases of kiwifruit. The disease is infamously referred to as Kiwifruit bacterial canker (KBC), a notable pandemic disease. Strikingly, this problematic pathogen exerts its deleterious effect on the host plant on a global scale as all the plant tissues get infected. Physiognomically, the infected kiwifruit has cankered branches, reddish-brown, spots on leaves, and flower rot, all of which depict the severity of KBC, making it a major threat to the global kiwifruit industry (Stonehouse *et al.* 2013; Vanneste *et al.* 2014; Kim *et al.* 2017; Donati *et al.* 2020). The population structure of *Psa* varies significantly depending on the species and environment that have prompted the uncovering of biovars (Fujikawa and Sawada 2019). Currently, *Psa* is classified into 5 biovars (biovar 1, 2, 3, 5, and 6), which are determined by genetic features and biological traits, including virulence and toxin production. Among these, *Psa* biovar 3, has been associated with severe outbreaks of bacterial canker in major kiwifruit production countries, namely Italy, New Zealand, Chile, and China (Butler *et al.* 2013). The pathogenicity of *Psa* M228 is dependent on its type III secretion system (T3SS), which directly injects virulence effectors into plant host cells to interfere with the host defense system. This nanomolecular machinery, T3SS is encoded by a group of genes known as hypersensitive response and pathogenicity/hypersensitive response conserved (*hrp/hrc*) genes that form a cluster. HrpL, a key regulator of T3SS, binds to a highly conserved "*hrp*-box" (GGAACC-$N_{15/16}$-CCACNNA) in the promoter to activate the expression of target genes (Xiao *et al.* 1992; Shen and Keen 1993; Xiao and Hutcheson 1994). The expression of *hrpL* is controlled by HrpR and HrpS, which are encoded by a single *hrpRS* operon. It has been reported that two-component signaling systems (TCSs) RhpRS (Xie *et al.* 2019b), CvsRS (Fishman *et al.* 2018), and GacAS (O'Malley *et al.* 2019; O'Malley *et al.* 2020), can regulate the *hrpRS* operon at the transcription level. However, the question of whether there are other unreported two-component signaling systems that can modulate the *hrpRS* operon has not been addressed. TCSs are crucial bacterial regulatory factors that control gene expression in response to environmental cues. In a two-component signaling system, histidine kinase serves as a sensory receptor for signal molecules, responsible for monitoring specific stimuli or stress factors from the host or the environment. Then, it transfers the phosphate group to the corresponding Response Regulator protein, activating its function and ultimately enabling a response to external environmental stimuli (Xie *et al.* 2019a). The RegAB system is a key regulator of energy-related cellular processes across different bacterial species, demonstrating its versatile functions. For example, in *Rhodobacter capsulatus* and *R. sphaeroides,* the RegAB system is involved in numerous metabolic pathways, encompassing

fundamental processes that utilize energy, such as photosynthesis and carbon metabolism, as well as processes that generate energy, exemplified by aerotaxis (Elsen *et al.* 2004). Recently, it was established that RegAB modulates anaerobic metabolism in *Burkholderia pseudomallei*, playing an important role in the nitrification process. The complex interaction of the RegAB-driven response is critical for achieving pathogenicity. (Phenn *et al.* 2021). In an independent study, Zhang *et al* (Zhang *et al.* 2023) did find that the RegAB regulatory system of anammox bacteria enhances the expression of the cbb3-type cytochrome c oxidase (CcO) commensurate with photosynthesis. The detailed analysis of the mechanisms through which RegAB activates and inhibits various phenotypes has shown that RegA binds to a consensus sequence of 5'-G(C/T)G(G/C)(G/C)(G/A)NN(T/A)(T/A)NNC(G/A)C-3' (Swem *et al.* 2001). The phenotypes and diverse mechanisms justify that RegA functions as a global regulatory transcription factor, regulating multiple operons such as those related to photosynthesis and respiratory electron transfer. It achieves this by binding to the promoter sequences of these operons to modulate their expression. However, the specific mechanism through which RegAB regulates the expression of the *Psa* T3SS remains incompletely elucidated.

In this study, we identified a two-component signaling system, kinase RegB (CN228_RS04480, GenBank accession: AYL79284.1), and its downstream regulatory transcription factor, RegA (CN228_RS04485, GenBank accession: AYL79285.1), as key regulators of T3SS expression and various biological processes in *Psa* M228. Here we report that RegA directly binds to the *hrpR* promoter, leading to the inhibition of *hrpR*/*S* gene transcription. Additionally, the phosphorylated RegA exhibits a higher binding capacity with the promoter. These findings provide valuable insights into the regulation of T3SS expression and pathogenicity by RegAB, laying the groundwork for understanding the pathogenic mechanisms of *Psa*.

2. Materials and methods

2.1. Bacterial strains, plasmids, media, and growth conditions

The bacterial strains and plasmids used in this study are listed in Appendix A. *Psa* M228 and various mutants were grown at 26℃ with shaking at 220 rpm in Luria-Bertani (LB) broth or on LB agar plates. If necessary, the bacteria were then centrifuged and washed three times with HDM solution (50 mM KH_2PO_4, 7.6 mM $(NH4)_2SO_4$, 1.7 mM $MgCl_2$, 1.7 mM NaCl, and 10 mM fructose, pH=5.8) before being cultured to reach optical density at 600 nm (OD_{600}) of 0.6 in HDM for 6 hours (Yang *et al.* 2008). *Escherichia coli* strains namely BL21 (DE3), TG1, and S17-1 were grown in LB medium at 37℃.

When required, antibiotics were added to the culture at the listed concentrations: ampicillin (Amp, 10 μg mL^{-1}), kanamycin (Km, 100 μg mL^{-1}), gentamicin (Gm, 10 μg mL^{-1}) and nalidixic acid (Ni, 5 μg mL^{-1}). All the primers used are listed in Appendix B.

2.2. Genetic methods

Gene deletion mutants of *Psa* were constructed by homologous recombination method utilizing the previously described suicide plasmid pK18mobsacB (Kvitko and Collmer 2011). Briefly, the gene fragments including their upstream and downstream arms were amplified using the corresponding primers (Appendix B). The resulting DNA fragments were digested with *BamH*I/*EcoR*I and ligated to pK18mobsacB. Then, pK18mobsacB recombinant constructs were introduced into the *Psa* M228 strain by conjugal mating experiments. The transformants were plated on LB (Km_{10}-Ni_{10}-Amp_{10}) agar plates (LB with 10 μg mL^{-1} kanamycin, 10 μg mL^{-1} nalidixic acid, and 10 μg mL^{-1} ampicillin) and incubated at 26℃ for 2-3 days. Primers *sacB*-F/R and *Psa*-F/R (Appendix B) were used to detect the transformants. The single colonies on sucrose plates were then cultured on plates with either the combination of 10 μg mL^{-1} Km and 10 μg mL^{-1} Amp or 10 μg mL^{-1} Amp alone to remove the suicide plasmid. All newly constructed deletion strains were confirmed by PCR amplification. Complement mutants were constructed as follows: The full-length sequences of the mutated genes with intact upstream putative promoters were amplified from the *Psa* M228 genome. The PCR products were cloned into the *BamH*I and *Kpn*I sites of plasmid pBBR1-MCS5. The plasmid constructs were transformed into *E. coli* DH5α. The complementation plasmids were extracted from *E. coli* DH5α using the Plasmid Mini Kit I (OMEGA, USA) following the manufacturer's instructions without any modification. The empty vector pBBR1-MCS5 and complementation plasmids were transformed into respective strains. The complement strains were screened by Gm resistance on LB agar.

2.3. Protein expression and purification

To express His_6-tagged proteins, each plasmid pET28a with the coding region of the gene of interest was transformed into *E. coli* BL21 (DE3) and cultured at 37°C in LB medium until reaching an OD_{600} of 0.5. Induction with 0.1 mM IPTG followed for an additional 12 hours at 16°C. Bacterial cultures were harvested by centrifugation at 8000 rpm for 3 minutes at 4°C, then resuspended in a lysis buffer (20 mM Tris-HCl, pH 8.0; 300 mM NaCl). Cell lysate was obtained through ultrasonication and centrifugation at 8000 rpm for 40 minutes at 4°C. The resulting supernatant was loaded onto a Ni-NTA column (Qiagen, China), according to the manufacturer's instructions. Purified recombinant proteins

were dialyzed overnight at 4°C in an appropriate buffer and stored at -80°C. Purity was assessed by SDS-PAGE, and their concentrations were determined using the Bradford assay (Kruger 1994).

2.4. Promoter activity assay

The *hrpL* and *hrpR* promoter activities were measured using the promoterless *luxCDABE* operon in the low-copy-number plasmid pMS402 as described earlier (Duan *et al.* 2003). The DNA sequence of *hrpL* and *hrpR* promoter was amplified and ligated into the pMS402 plasmid. The *lux* reporter fused with promoters of *hrpL* or *hrpR* were transformed into the *Psa* M228 strains and cultured in LB medium to OD_{600}=0.6. Then, the cultures were washed three times with HDM medium and incubated 6 hours in HDM. A 200 μL culture was then transferred to a black 96-well plate with a transparent bottom. Promoter activities were measured using a Synergy 2 Plate Reader (BioTek, USA), the expression of the *luxCDABE* operon from bacteria grown in liquid culture was measured as counts per second (cps) of light production. Bacterial growth was monitored at the same time by measuring the OD_{600}.

2.5. Measurement of *Psa* M228 growth rate

To investigate the impact of different strains on the growth of *Psa* M228, single colonies of *Psa* M228 were collected in 5 mL LB liquid medium and incubated at 28℃ and 220 rpm. Once the cultures reached an OD_{600} of 1.0, the cells were transferred to 100 mL liquid LB medium at a ratio of 1:100. The growth of the bacterium was monitored every 3 hours over a 24-hour period until reaching the stable phase.

2.6. Pathogenicity tests

The pathogenicity of the related strains was evaluated using a leaf-disc inoculation assay as described earlier (Zhao *et al.* 2019). Following surface disinfection of leaves, leaf discs were created using a hole punch (11 mm diameter), taking care to avoid open veins. These leaf discs were then immersed in a bacterial solution with a concentration of 10^4 CFU mL^{-1} using vacuum infiltration at 0.1 MPa for 10 seconds, repeated three times. Subsequently, the leaf discs were washed three times with sterile water and placed on 0.5% water agar plates. The plates were incubated in a climatic chamber with a 16 hours light cycle at 18°C and an 8 hours dark cycle at 16°C. Photographs of the leaf discs were taken 7 days post-inoculation (dpi). After 5 days of inoculation and culture, the surface water of the leaf disc was blotted using absorbent paper. The Image J software was then utilized to compare the lesion area of each leaf disc. Following the removal of leaf disc data with significant errors in the sample, the average incidence rate was calculated.

2.7. RNA extraction and qRT-PCR analysis

Psa M228 and its mutant strains were cultured in LB medium until reaching an OD_{600} of 0.6, followed by transfer to HDM for an additional 6 hours as needed. Bacterial cells were then harvested through centrifugation. Total RNA was extracted using the RNA prep Pure Cell/Bacteria Kit (Tiangen Biotech, Beijing, China) and treated with DNase I (Sigma, Germany). Subsequently, cDNA was generated utilizing the Trans Script II One-Step gDNA Removal and cDNA Synthesis Super Mix (TransGen Biotech, Beijing, China), and subjected to qRT-PCR with the KAPA SYBR FAST qPCR Kit (Kapa Biosystems, USA) in a Light Cycler 96 thermocycler (Roche, Switzerland). The reference gene used for normalizing mRNA levels was *gyrB* (DNA gyrase subunit B). Experiments were conducted in triplicate for each strain.

2.8. Bacterial two-hybrid assay

Bacterial two-hybrid assays were carried out as previously described (Karimova *et al.* 1998). Briefly, *E. coli* BTH101 competent cells were co-transformed with bait and prey plasmids, followed by selection on LB plates containing ampicillin and kanamycin. The resulting colonies were then plated on MacConkey plates supplemented with IPTG and maltose, and incubated at 30°C. Interactions between different hybrid proteins were quantified by measuring β-galactosidase activity in liquid cultures. Specifically, overnight cultures were diluted to 1%, grown in LB broth with antibiotics at 37°C, and harvested at an OD_{600} of 1.5. Subsequently, cells were permeabilized using chloroform and SDS, and β-galactosidase activities were assayed with o-nitrophenyl-/3-D-galactoside (ONPG) as the substrate, following the protocol (Giacomini *et al.* 1992). All experiments were performed at least three times independently.

2.9. Hypersensitive Reaction Assays

HR assays were performed with *Nicotiana benthamiana* as described previously (Zhao *et al.* 2022). Wild-type M228 and its derivative strains were cultivated until reaching an OD_{600} of 1.0. Bacterial suspensions were then adjusted to a concentration of 10^8 CFU mL^{-1} in a 10 mM $MgCl_2$ buffer, and subsequently infiltrated into tobacco leaves using a blunt-ended plastic syringe with a penetration diameter of approximately 1 cm. The leaves were examined for HR lesions twenty-four hours post-inoculation. A staining solution, heated to 95°C, was combined with trypan blue (0.67 mg mL^{-1}) for 5 minutes. Chloral hydrate (2.5 mg mL^{-1}) was introduced to bleach the solution, with changes made every 2 hours. The outcomes were documented by capturing images of the leaves after complete bleaching.

2.10. Electrophoretic mobility shift assay (EMSA)

EMSA was performed as described with minor modifications (Song *et al.* 2015). Briefly, 230 bp upstream regions of *hrpR* DNA probes containing the binding site were amplified using primers P_{hrpR}-F and P_{hrpR}-R. As a negative control, a 240 bp fragment from the *hrpR* coding region was amplified using primers control-F/control-R, and 1 μM BSA was included in the binding assay. The assay mixture was prepared according to the manufacturer's instructions (Light Shift® Chemiluminescent EMSA Kit, Thermo, USA) and consisted of 50% glycerol, 100 mM $MgCl_2$, 1% NP-40, 1 M KCl, 200 mM EDTA, 20 ng DNA, and 10×binding buffer (100 mM Tris, 500 mM KCl, 10 mM DTT; pH 7.0). Following a 30-minute incubation at room temperature, the binding reaction mixture was analyzed by electrophoresis on a 6% native polyacrylamide gel containing 5% glycerol in 0.5×TBE (Tris-borate-EDTA) electrophoresis buffer at 100 V, and the DNA probe was detected using SYBR Green.

2.11. MST assay

The protein-DNA interaction was determined by MST using a Monolith NT.115 (NanoTemper Technologies, Germany) as described earlier (Su *et al.* 2017). For the MST binding assay, the purified GST-RegA and GST were specifically labeled with the fluorescent dye RED-NHS (NanoTemper Technologies, Germany). A constant concentration (2 μM) of the labeled target protein in a standard MST buffer (50 mM Tris, pH 7.5, 150 mM NaCl, 10 mM $MgCl_2$ and 0.05% Tween 20) was titrated against increasing concentrations of *hrpR* promoter from 100 μM to 1.56 nM. The MST premium coated capillaries (Monolith NT.115 MO-K005, Germany) were used to load the samples into the MST instrument at 25°C using medium MST power and 60% LED power. The Fraction Bound was plotted on a linear y-axis against the total concentration of the titrated partner on a log10 x-axis. All the experiments were performed in triplicate. The data were analyzed using Nanotemper Analysis software v.1.2.101 (NanoTemper Technologies).

2.12. Transcriptome analysis

Wild-type *Psa* M228 and *regA* mutant strains were cultivated at 26°C with shaking at 220 rpm in LB medium until reaching an OD_{600} of 0.6. Subsequently, they were washed twice with HDM medium and transferred to HDM at 16°C for 6 hours. The bacteria were then harvested by centrifugation, and total RNA was extracted. A cDNA library was constructed through a series of steps including reverse transcription, end preparation, adaptor ligation, and PCR amplification using the RNA samples. The

final libraries were sequenced on an Illumina HiSeqTM 2000 platform (GENE DENOVO-Guangzhou, China). Following this, low-quality reads were filtered out, and the remaining clean reads were aligned to the reference genome of *Psa* M228 (NCBI: CP032631.1) using BWA alignment (Li and Durbin 2010). RESM and NOISeq tools were employed to normalize gene expression levels and identify differentially expressed genes (DEGs) between the wild-type *Psa* M228 and the mutant strain (Wang *et al.* 2017). The DEGs identified were further analyzed for enrichment using the Kyoto Encyclopedia of Genes and Genomes (KEGG) pathway and KEGG Orthology (KO) metabolic pathway databases (Kanehisa *et al.* 2008).

2.13. Statistical Analysis

GraphPad Prism 8 (GraphPad Software, San Diego California, USA) was used for data analysis and graphing. Statistical analyses for the rest of the assays were performed using paired two-tailed Student's t-test. Error bars represent ± SD. **P*<0.05; ***P*<0.01; ****P*<0.001.

3. Results

3.1. RegAB negatively regulates bacterial virulence

RegAB is a pair of two-component signaling system widely present in bacteria. RegB is an orthodox histidine kinase (HK), containing a histidine phosphotransfer (DHp) domain and a catalytic histidine kinase (CA) domain. RegA is a Fis-family transcription factor (TF) that has an N-terminal receiver domain and a C-terminal DNA binding domain (Fig. 1-A). Reverse transcription PCR (qRT-PCR) analysis was used to dissect the structure of the RegAB operon. As shown in Appendix C-A, using cDNA as a template obtained a product that corresponded to the using Genomic DNA as a template between *regB* and *regA*. This result supported the view that RegB and RegA form a bicistronic operon and are under the control of the same cis-regulatory elements. To determine the function of RegAB in *Psa* pathogenicity, leaf discs were vacuum infiltrated with 10^4 CFU mL^{-1} of the *regA* and *regB* deletion mutant, with H_2O used as a negative control. Pathogenicity of the deletion mutants was significantly enhanced compared to the wild-type M228, whereas pathogenicity of the complementation strains Δ*regA*(*regA*) and Δ*regB*(*regB*) showed no significant difference from the wild-type M228 (Fig.1-B and 1-C). To investigate the effect of RegAB on the growth of *Psa* M228, the growth curves of Δ*regA and* Δ*regB* mutants were measured. The results indicate that neither the Δ*regA* nor the Δ*regB* mutant displayed growth defects compared to the wild-type strain WT(pBBR) (Appendix C). The T3SS is a key factor in the virulence of *Psa,* often triggering hypersensitive reaction (HR) production in

nonhost plants. To investigate the impact of RegAB on HR induction in *N. benthamiana*, the wild-type M228, Δ*regA*(pBBR) and Δ*regB*(pBBR) mutants and the corresponding overexpression strains WT(*regA*) and WT(*regB*) were separately injected into *N. benthamiana* plants. Subsequently, leaf necrosis was observed and stained with trypan-blue dye after 24 hours. Quantitative comparisons of the lesion area showed that the ability of Δ*regA*(pBBR) or Δ*regB*(pBBR) to stimulate *N. benthamiana* HR was significantly enhanced than the wild type WT(pBBR) (Fig. 1-D and 1-E).

3.2. RegAB regulates multiple physiological pathways in *Psa* M228

RegA has a REC domain that receives phosphorylated signals, as well as a helix-turn-helix (HTH) DNA-binding domain. To further understand the mechanism whereby RegAB inhibits the pathogenicity of *Psa*, we conducted RNA-sequencing (RNA-seq) to compare the transcriptomic profiles of the Δ*regA* mutant with the wild-type M228 strain. A total of 472 differentially expressed genes with more than absolute 1.0-$\log_2$fold change were identified between these two strains (Appendix D). KEGG enrichment analysis of these genes revealed significant involvement in bacterial secretion systems, carbon metabolism, plant-pathogen interactions, and photosynthesis (Fig. 2-A). Notably, genes linked to bacterial virulence and oxidative phosphorylation, including F-type ATPase, were identified. These findings align with previous studies on the regulatory roles of RegAB in energy processes (Elsen *et al.* 2004). Meanwhile, other differentially expressed genes are involved in bacterial pathogenicity, motility, two-component signaling system AauRS, and quorum sensing, which have not been reported yet (Fig. 2-B).

3.3. RegAB regulates multiple physiological pathways in *Psa* M228

The expression of T3SS cluster genes were found to be fully regulated by RegA. The analysis of transcriptome data revealed that gene transcripts within the T3SS operon exhibited an average regulatory increase of 1.85-4.97 folds in Δ*regA* (Fig. 3-A). Particularly, the expression level of *hrpL*, which serves as the main controlling factor for T3SS activity, was increased by 4.6 fold. Furthermore, upon analyzing 19 type III effector (T3E) genes, it was observed that the expression levels of most genes significantly increased in Δ*regA* (Fig. 3-B). These results indicate that RegA negatively influences the transcriptional activation of the T3SS gene expression.

Quantitative reverse transcription PCR (qRT-PCR) was used to detect the mRNA levels of *hrpL*, *hrp* cluster (*hrcS*, *hrcN*, *hrcU*), and type III effector protein (T3E) genes (*avrE1* and *hopR1*). The results showed significant upregulation of each gene in mutation compared to the wild-type (Fig. 3-C),

indicating an inhibitory effect of RegAB on T3SS transcriptional activity. Additionally, luciferase reporter activity analysis confirmed the increased expression of *hrpL* (Fig. 3-D). These findings highlight the role of RegAB expression in the pathogenicity of *Psa* M228. Overall, the data indicates that RegAB plays a partial role in controlling virulence by modulating the expression of T3SS genes.

3.4. RegA binds to the promoter of *hrpR*/*S* operon

Previous studies across different species have shown that the regulatory response protein RegA functions as a transcriptional regulator by interacting with downstream promoters to affect gene expression. Through an analysis of existing literature and promoter sequence information, a specific 9-base pair sequence (Appendix E-A) associated with RegA binding (Elsen *et al.* 2004) was identified. This sequence was then used in our sequencing analysis of the *Psa* M228 genome by Find Individual Motif Occurrences (FIMO). This study identified an additional promoter, the promoter region of *hrpR*, as a potential RegA binding site. The motif identified in the *hrpR* promoter had a p-value of $6.53E^{-8}$. A RegA-protected site (GCTGCGGGG) was found upstream of the -35 and -10 elements (Appendix E-B). EMSA confirmed that RegA binds to the promoter region of *hrpR* (Fig. 4-A). Using MST, we found that GST-RegA could bind to the promoter region of *hrpR* with a moderately high affinity (K_d, 0.47 μM). Importantly, the GST tag itself did not bind to the promoter region of *hrpR* (Fig. 4-B). To determine if *hrpR* is a direct regulon of RegA, qRT-PCR was performed to assess the mRNA level of *hrpR* in the Δ*regA*(pBBR) or Δ*regB*(pBBR) mutant strain. The results indicated a significant increase in the expression of *hrpR* in both mutant strains compared to the wild-type M228(pBBR). However, transcription of *hrpR* was decreased in the complementation strains Δ*regA*(*regA*) and Δ*regB*(*regB*) (Fig. 4-C), and this result is supported by the data of *lux* reporter activity assay (Fig. 4-D). Together, these results indicate that RegA acts as a repressor of *hrpR* in *Psa* M228.

3.5. The phosphorylation is required for RegA to repress T3SS gene transcription

The REC domain of the *Psa* RegA contains a conserved aspartate residue, Asp64 (D64) (Appendix F-A), which is presumed to undergo phosphorylation by the histidine kinase RegB (Phenn *et al.* 2021). To investigate the impact of phosphorylation on DNA binding, we created two RegA variants. One variant, $RegA^{D64A}$, was anticipated to be inactive, while the other variant, $RegA^{D64E}$, was expected to be constitutively active, simulating the phosphorylated state. The binding affinity of both RegA variants to P_{hrpR} was assessed using EMSA. The results of the EMSA demonstrated that RegA and $RegA^{D64A}$ displayed the same binding affinity to the *hrpR* promoter at equivalent protein concentrations, whereas

RegA^{D64E} enhanced binding (Fig. 5-A). These findings indicate that phosphorylation plays an important role in RegA binding with the *hrpR* promoter.

Genetic and phenotypic assays were conducted to assess the physiological relevance of the biochemical analyses mentioned previously. Deletion of the *regA* gene led to an increase in *hrpR* mRNA levels, indicating that RegA binding down-regulates *hrpR* expression. This defect was rescued by complementation with the native *regA* or the constitutively active *regA*^{D56E} in the Δ*regA* strain, but not complementation with the inactive *regA*^{D56A} (Fig. 5-B), and this result is supported by the data of *lux* reporter activity assay (Appendix F-B). Together, these results suggest that phosphorylated RegA acts as a repressor of *hrpR* in *Psa* M228. HrpR is a transcriptional regulator known to positively regulate T3SS gene expression and pathogenicity in *Psa*. To investigate the relationship between the regulation of RegA pathogenicity and its phosphorylation, we analyzed the expression of T3SS-related genes in *Psa* M228 and its derivative strains. Our results indicate that complementation with *regA* and *regA*^{D64E} (a constitutively active mutation where Asp is converted to Glu) leads to a decrease in mRNA levels of *hrpL*, *hrcS,* and *hopR1* to levels similar to the wild-type M228. However, the Δ*regA*(*regA*^{D64A}) strain did not show this decrease in gene expression (Fig. 5-C). These findings imply that the phosphorylation of RegA is essential for the repression of T3SS genes.

Initial observations suggest that phosphorylation of RegA is necessary for the repression of T3SS genes. To further investigate the role of phosphorylation in bacterial pathogenicity on host plants and HR in nonhost plants, we examined the strains Δ*regA*(*regA*^{D64A}) and Δ*regA*(*regA*^{D64E}). The inactive strain Δ*regA*(*regA*^{D64A}) exhibited a higher incidence rate compared to the wild-type strain, while the constitutively active strain Δ*regA*(*regA*^{D64E}) had a lower incidence (Fig. 5-D and Fig. 5-E). This indicates that phosphorylation of RegA could decrease bacterial pathogenicity. Additionally, the ability of Δ*regA*(*regA*^{D64A}) to induce *N. benthamiana* HR was significantly higher than that of the wild-type M228(pBBR), while the ability of Δ*regA*(*regA*^{D64E}) to induce *N. benthamiana* HR was lower than that of the WT(pBBR) (Fig. 5-F). These findings indicate that phosphorylation of RegA is crucial for its role in the pathogenicity of *Psa* M228 in host plant and hypersensitive reaction (HR) in nonhost plant.

4. Discussion

The pursuit of virulence mechanisms in *Psa* not only advances understanding of molecular underpinnings but prompts the identification of targets for intervention in managing pandemic outbreaks of KBC. Genetic factors that modulate T3SS activity provide crucial insights into the pathogenicity of

Psa. In this study, we employed genetic techniques, biochemical approaches, and a microbe-plant model to explore the role and mechanisms of functionally uncharacterized TCS in regulating the pathogenicity of *Psa*. For the first time, RegAB was shown to regulate a virulence phenotype, T3SS of *Psa*. Specifically, HK RegB sensed an unknown signal to enhance the phosphorylation level of RegA, occasioning a high binding affinity of the latter for the promoter of the *hrpR*/*S* operon, thus repressing *hrpR*/*S* and other T3SS-related gene expression. To better summarize the major findings of this current study, we have developed a schematic model dubbed the RegAB-HrpRS-T3SS pathway, elucidating the mechanism of RegAB in the regulation of pathogenicity (Fig. 6). Additionally, we found RegAB is implicated in regulating various biological processes in *Psa* M228. These results contribute to our understanding of the TCS function in *Psa* and provide a basis for the advancement of RegAB-dependent molecular regulatory mechanisms.

Previously, the RegAB system in *Mycobacterium smegmatis*, which is not related taxonomically and occupies different ecological niches from *Psa*, played a crucial role as a global regulator of various energy-generating and energy-utilizing cellular processes (Maarsingh *et al.* 2019). The processes monitored by the RegAB system include key functions such as photosynthesis, carbon dioxide fixation, nitrogen assimilation, hydrogen utilization, denitrification, dehydrogenases, electron transport, and aerotaxis (Phenn *et al.* 2021). Facilitated by high-throughput RNA-seq analysis, we discovered the two-component signaling system RegAB is also involved in regulating carbon metabolism, oxidative phosphorylation, and electron transport in *Psa* M228 (Fig 2-A); this is consistent with previously reported findings (Elsen *et al.* 2004). Additionally, RegAB was found compromised in bacterial virulence, particularly in bacterial secretion systems such as T3SS, as well as in plant-pathogen interactions that have not yet been documented (Fig. 2-B). This highlights the direct involvement of the RegAB system in the regulation of virulence genes in pathogens, which plays a significant role in pathogenesis.

RegA has been shown to bind to various operons such as *nifA2*, *hupSLC*, *petABC*, *cycA, cycY, cydAB, cbbI*, and *cbbII* (Dubbs *et al.* 2000), demonstrating that RegA directly influences carbon fixation by binding to specific sites in the *cbbI* and *cbbII* promoters in *R. sphaeroides*, which are notably GC-rich. Experimental data indicate that RegA exhibits a preference for a GCG...CGC palindromic sequence. The RegA binding sequences were identified using the Multiple Em for Motif Elicitation (MEME) website and visualized through a sequence logo (Appendix F). Analysis of the *Psa* M228

genome revealed a RegA binding site GCTGCGGGG upstream of the *hrpR* promoter, confirmed by EMSA and MST experiments (Fig. 4-A and Fig. 4-B). Consistent with previous findings, RegA is known to regulate operon expression within the RegAB regulon by binding to relevant promoters.

Two-component kinases play a crucial role in sensing the external environment and regulating the phosphorylation of downstream response-regulating proteins to modulate biological responses (Xie *et al.* 2019a). In *P. syringae*, the expression of the key T3SS mechanism that affects disease severity is controlled by various two-component signaling systems. These include TCS CvsRS, which detects metal ions (Fishman *et al.* 2018), TCS AauRS, which responds to aspartate and glutamate (Anderson *et al.* 2014; Yan *et al.* 2020), which responds to aspartate and glutamate, and the photosensory system LOV-HK (Cao *et al.* 2008; Moriconi *et al.* 2013). Our research has discovered a new two-component signaling system RegAB that directly targets *hrpR*/*S* to regulate T3SS. Unfortunately, physiologically relevant signals of RegAB have not yet been identified, so it is still unclear how RegAB is activated or repressed in response to the host environment. RegAB was initially identified as essential for activating photosynthesis gene expression in anaerobic conditions (Sganga and Bauer 1992; Mosley *et al.* 1994). It is proposed that under hypoxic conditions, RegAB induces the expression of genes involved in anaerobic metabolism and other regulators (Phenn *et al.* 2021). Furthermore, RegB is suggested to be a response to redox signals beyond oxygen availability. When *R. capsulatus* is grown chemically autotrophically (e.g., in the presence of oxygen, hydrogen, and carbon dioxide), it can effectively alleviate the inhibition of pigment biosynthesis by RegAB (Abada *et al.* 2002). This implies that rather than being directly influenced by oxygen levels, RegB likely modulates its phosphorylation in response to the cellular redox state. Therefore, our forthcoming investigations will be directed toward elucidating how RegB senses variations in cellular redox status to activate downstream regulatory proteins.

5. Conclusion

The findings of this study indicate that the two-component signaling system RegAB functions as a novel regulator of T3SS. Specifically, RgeA was observed to directly inhibit the expression of two key T3SS regulator genes, *hrpR* and *hrpS*, thereby controlling virulence in a T3SS-dependent manner. Phosphorylation is highlighted as a key factor in RegA's repression function. Furthermore, RNA-seq analysis demonstrated that RegAB also influences various other physiological pathways, including those related to bacterial pathogenicity, motility, the two-component signaling system AauRS, and quorum sensing. These findings emphasize the diverse regulatory functions of RegAB in facilitating

host adaptation.

Acknowledgements

This study was supported by the Natural Key Research and Development Program (2022YFD1400200 to Wang Yao and Yang Ming-ming), National Natural Science Foundation of China (32330004 to Shen Xi-hui, 32170130 to Wang Yao and 32102283 to Yang Ming-ming). We thank Wang Ruo-lin for her technical assistance and He Yan-ting for providing *N. benthamiana* during the HR experiments. We would also like to thank our laboratory members Qian Xin-yu and Huang Jia-nan for their constant support and encouragement throughout this research.

Declaration of competing interest

The authors declare that they have no conflict of interest.

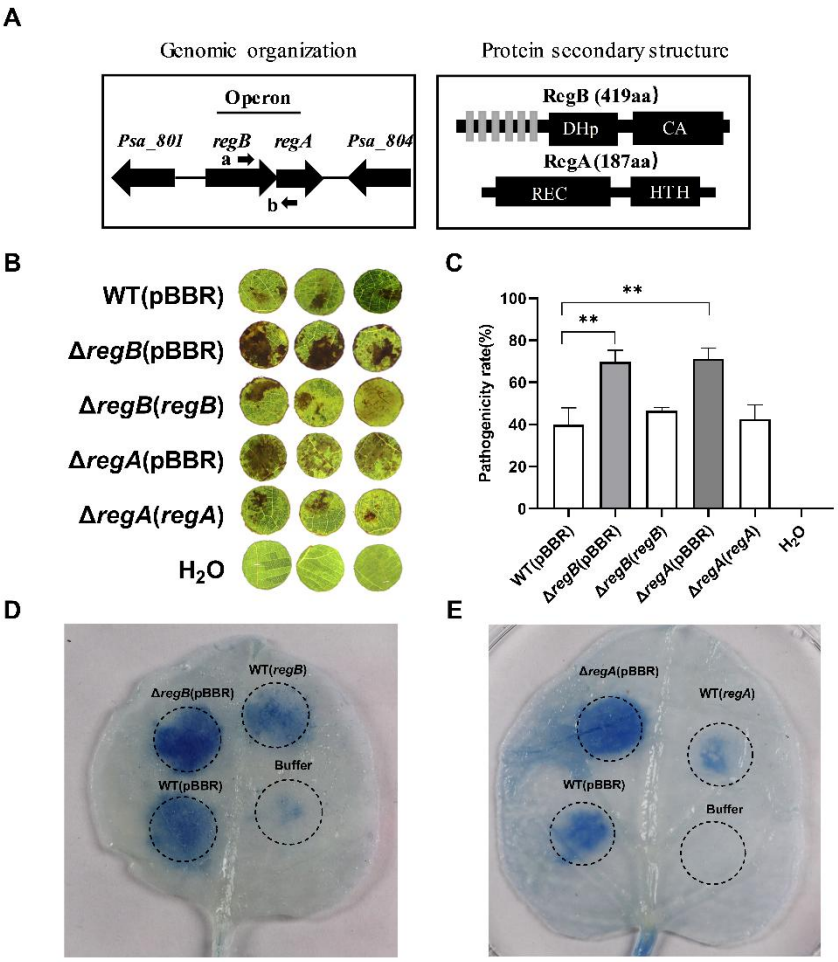

Fig 1. RegA/B negatively regulates bacterial virulence. (A) Schematic view of the genomic organization of the *regA-regB* locus and the putative secondary structures of their protein products. Upper panel: large black arrows indicate genes and their transcription directions. Small arrows indicate

the location of primers used for RT-PCR in Appendix C-A. Lower panel: the names of the protein domains are according to the Pfam database. HisKA = DHp: dimerization and histidine phosphotransfer domain; CA = HATPase_C: catalytic domain of histidine kinase; REC: receiver domain; HTH: helix-turn-helix domain. A gray frame indicates the transmembrane region of RegA. (B) The incidence rate and (C) percentage of incidence area of M228, *regA* or *regB* deletion mutant, and the corresponding complementary strains Δ*regA*(*regA*) and Δ*regB*(*regB*). Sterile water was used as a negative control. Error bars represent ± SD. ***P*<0.01. (D) and (E) Representative images of an *N. benthamiana* leaf after inoculation with wild type M228 and *regA* or *regB* deletion mutant, and the corresponding overexpression strains WT(*regA*) and WT(*regB*), DAB staining, and ethanol decolorization. Buffer (10 mM $MgCl_2$) was used as a negative control. WT(pBBR), wild-type strain M228 containing an empty vector; Δ*regA*(pBBR), the *regA* deletion mutant containing an empty vector; Δ*regB*(pBBR), the *regB* deletion mutant containing an empty vector; WT(*regA*), the wild type M228 containing a plasmid-borne *regA*; WT(*regB*), the wild type M228 containing a plasmid-borne *regB*.

A

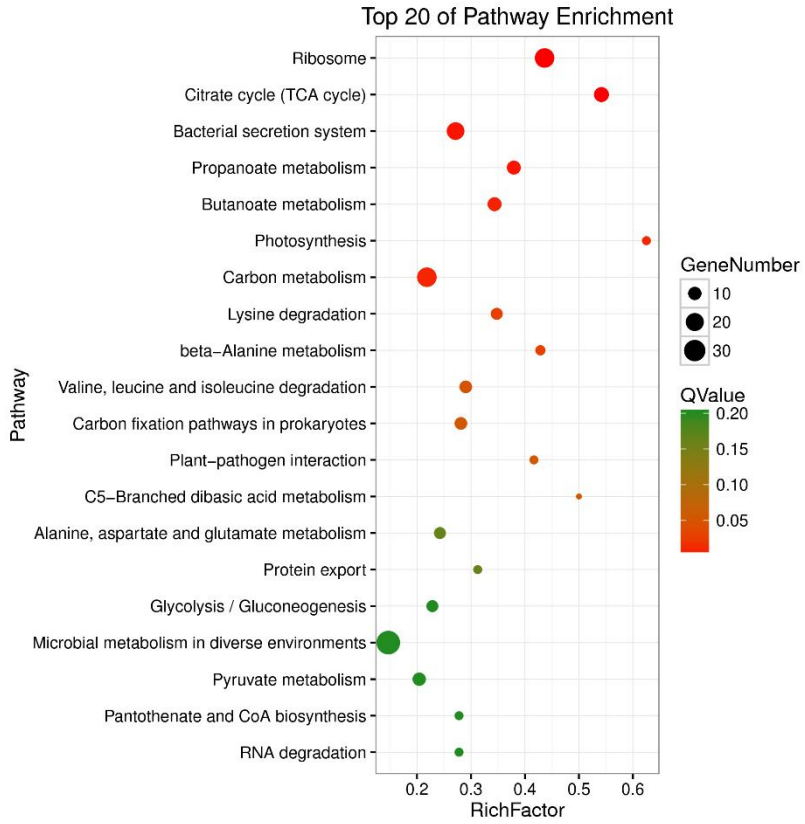

B

Gene family	Gene name or ID	Fold change
Bacterial secretion system		
Type II secretion system	*gspI, secB, secY, SRP54, yidC*	-1.92 to -2.7
Type III secretion system	*setC, hrcJ, hrpL, hrcN, hrcQ, hrcR, hrcS, hrcT, hrcU, hrcV*	2.32 to 4.60
Type VI secretion system	*hcp*	-1.98
Plant-pathogen interaction		
Bacterial secretion system	*yopJ, avrPto1, avrRpm1, avrXccC*	2.30 to 2.59
PAMP	*tuF*	-1.89
Oxidative phosphorylation		
Fumarate reductase	*sdhA, sdhB*	-1.95 to -2.03
F-type ATPase	*atpB, atpD, atpH, atpC, atpG*	-1.98 to -2.34
Cell motility		
Flagellum and pilus proteins	*flgK, flgJ, flgE, flgD, flgC, flgB, flgM, flgN, fliT, fliS, fliD, flaG, fliC*	1.02 to 1.97
chemotaxis	*mcp*	2.4
Quorum sensing	*rhlA, rhlB, rhlC*	-2.77 to -2.84
Biofilm formation	*pilL, fiS*	-2.03 to -2.23
Two-component system	*aauS, aauR, aatP, aatM, aatQ, aatJ*	12.34 to 125.00

Fig 2. RegA/B regulates multiple physiological pathways in *Psa* M228. (A) Enrichment analysis of the top 20 KEGG pathways of the differentially expressed genes (q value <0.2). (B) Selected gene families related to bacterial different metabolic pathways with more than 1.0-log2fold changes owing to the deletion of *regA* in *Psa* M228 (Δ*regA* versus WT).

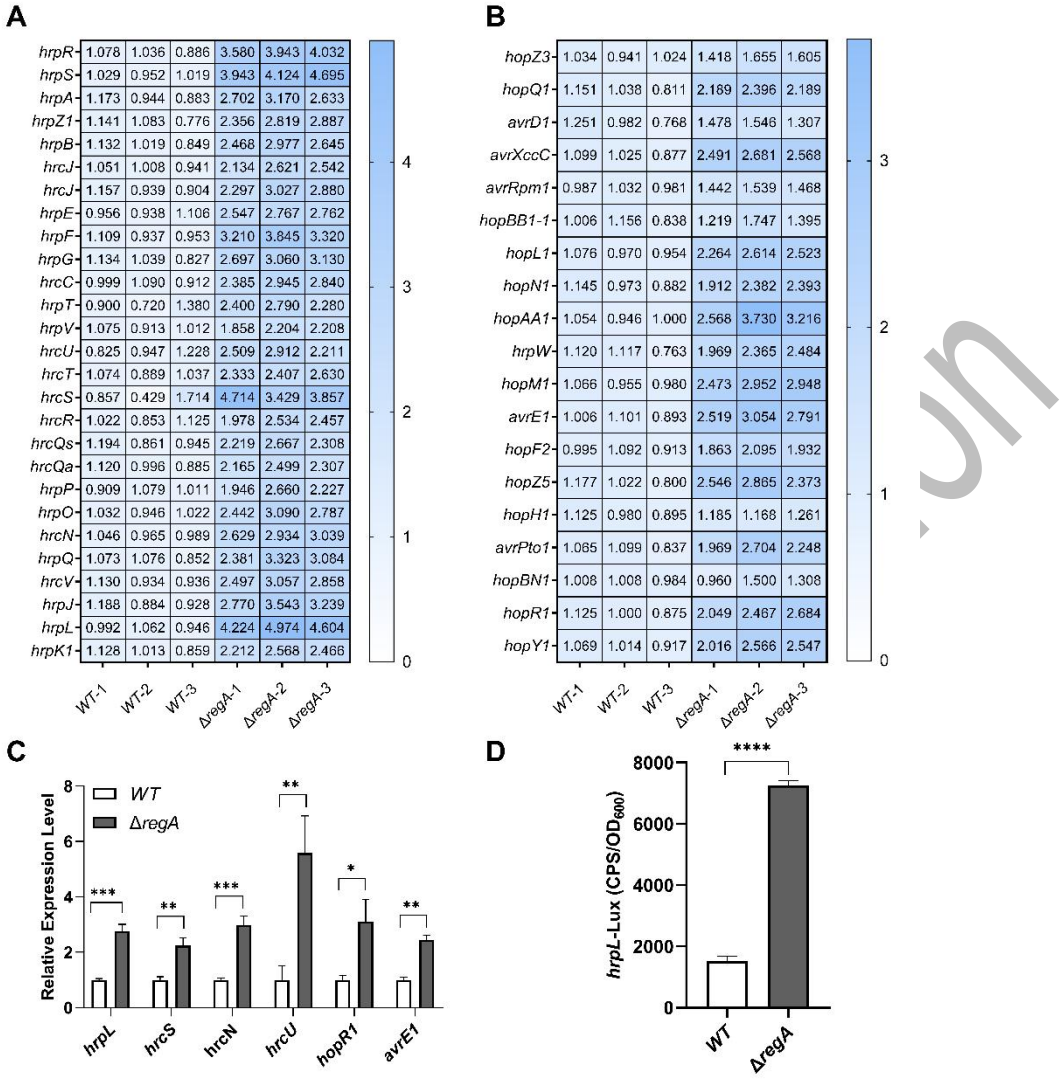

Fig 3. Effects of RegB on T3SS-Related Gene Expression. (A) Heat map of *hrp/hrc* genes expression in M228 and Δ*regA*. (B) Heat map of type III effector genes in M228, Δ*regA*. (C) The mRNA abundance of the T3SS-related gene was measured by quantitative reverse transcription PCR. The vertical bar indicates SD. **P*<0.05; ***P*<0.01; ****P*<0.001. (D) Luminescence of strains with pMS402-*lux* reporters driven by promoters of *hrpL*. Error bars represent ± SD. *****P*<0.0001.

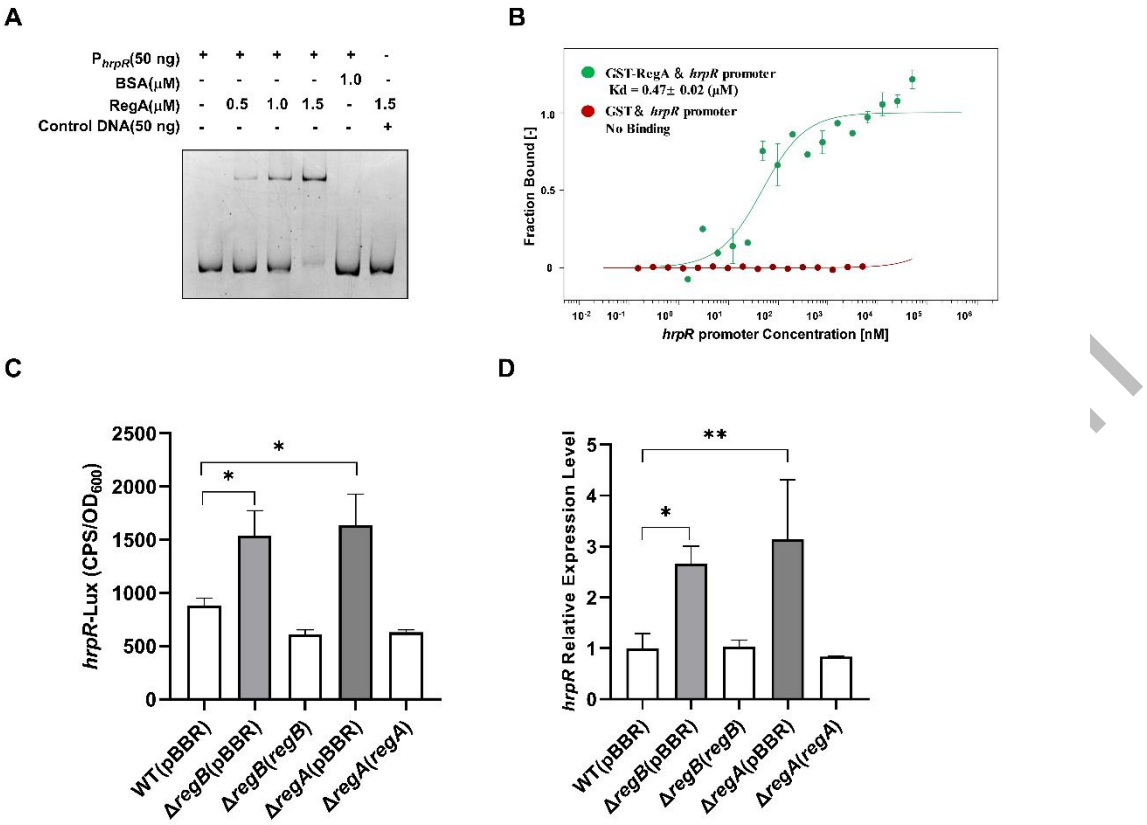

Fig 4. RegA binds to the *hrpR* promoter regions and represses the expression of T3SS. (A) EMSA validating binding of RegA to *hrpR* promoter regions. The BSA is used as a negative control. (B) MST validates the binding of GST-RegA to the *hrpR* promoter with a moderately strong affinity (K_d, 0.47 μM) and GST does not bind with the *hrpR* promoter. (C) qRT-PCR reveals that RegAB suppresses the expression of *hrpR*. The data shown is the mean ± SD of triplicate measurements, and *gyrB* was used as a control. **P*<0.05. (D) Luminescence of strains with pMS402-*lux* reporters driven by promoters of *hrpR*. The pMS402-*hrpR* was transformed into the wild-type strain, the Δ*regA*/*B* strain, and the complemented strain. A single colony was cultured in KB until it reached an OD600 of 0.6 and then transferred into HDM. After culturing for 6 hours, the luminescence value and OD600 were measured. * indicate significant differences between *regA* or *regB* mutants and wild-type. **P*<0.05; ***P*<0.01.

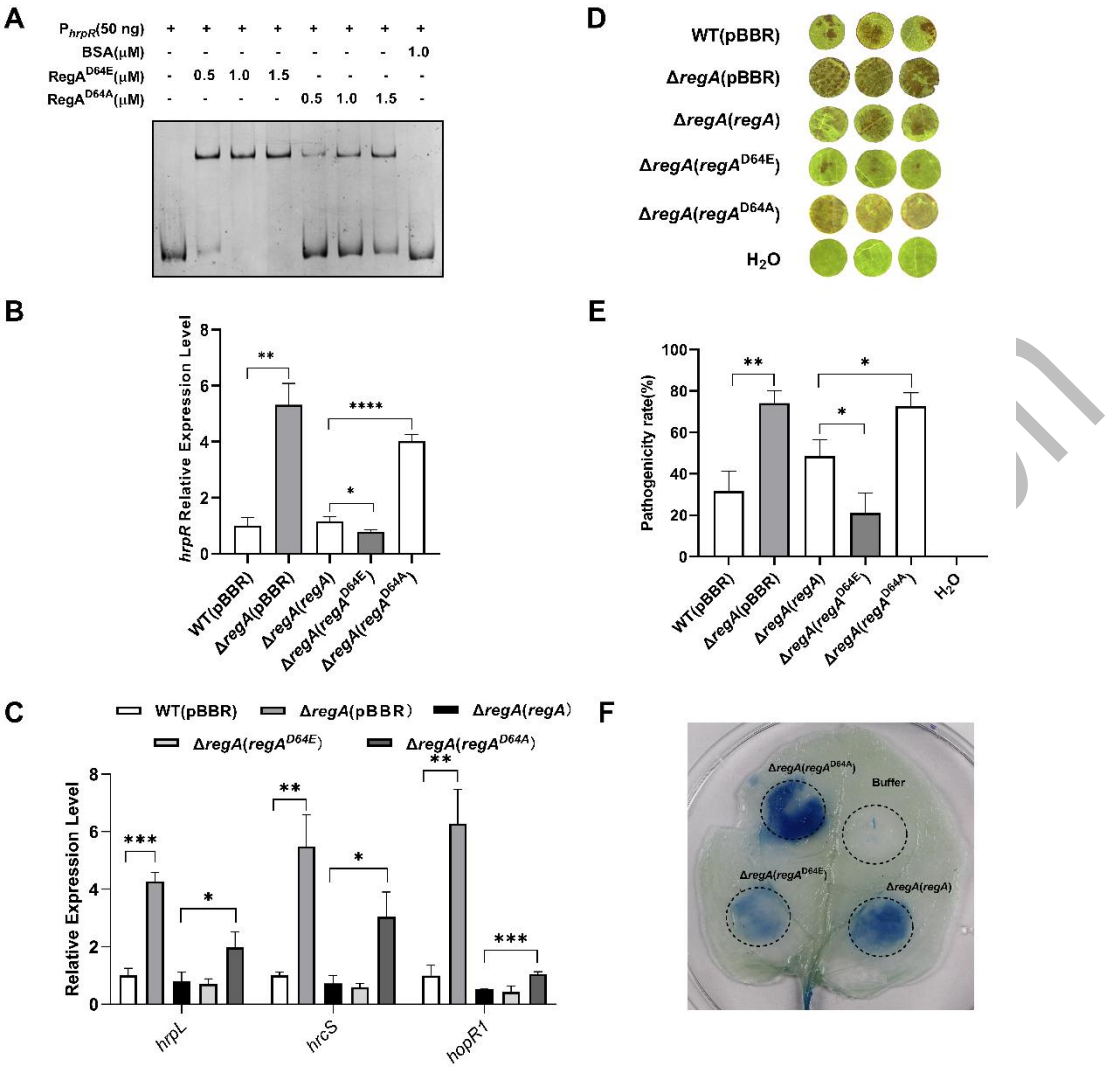

Fig 5. RegA negatively regulates T3SS expression based on phosphorylation. (A) RegA phosphorylation stimulates binding to P_{hrpR}, as measured by the electrophoretic mobility shift assay. The mRNA abundance of *hrpR* (B) and other T3SS-related genes (C) was measured by quantitative reverse transcription PCR. The leaf disc incidence (D) and percentage of incidence area (E) of wild-type M228 and its derivative strains. The vertical bar indicates SD. **P*<0.05; ***P*<0.01; ****P*<0.001; *****P*<0.0001. (F) Representative image of an *N. benthamiana* leaf after inoculation with wild-type M228 and its derivative strains. Buffer (10 mM $MgCl_2$) was used as a negative control. WT(pBBR), wild-type strain M228 containing an empty vector; strains Δ*regA*(*regA*), Δ*regA*(*regA*^{D64A}), and Δ*regA*(*regA*^{D64E}) contain plasmid-borne *regA*, *regA*^{D64A}, and *regA*^{D64E} respectively, in the Δ*regA* mutant.

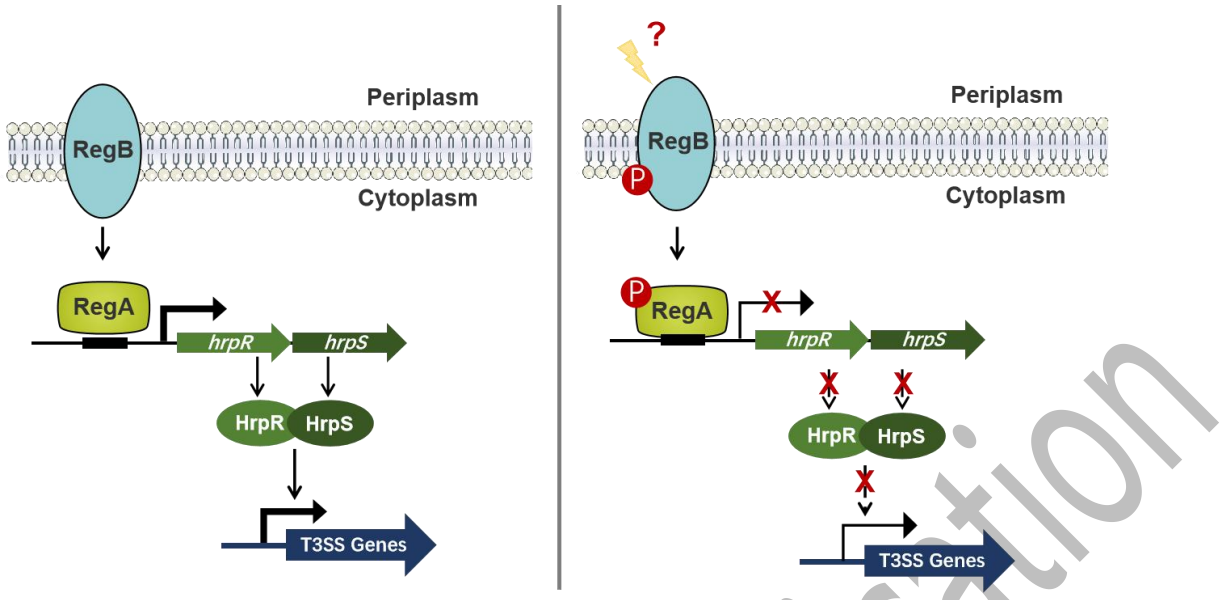

Fig 6. Proposed model of the RegAB-HrpRS-T3SS pathway. In the initial infection phase, *Psa* deploys histidine kinase RegB and response regulator RegA in a state of low phosphorylation. When RegA is in a low-phosphorylated state, it exhibits lower binding affinity with the *hrpR* promoter, allowing for the activation of downstream *hrpRS* which in turn activates the expression of T3SS genes. This upregulation of T3SS gene expression enhances the bacteria's ability to invade host plants. Upon infecting host cells, an unknown signal triggers the phosphatase activity of RegB, leading to increased phosphorylation of RegA. This elevated phosphorylation level of RegA has a high binding affinity with the *hrpR* promoter to repress the expression of the *hrpR*/*S* operon, subsequently suppreing the induction of downstream T3SS genes and reducing the virulence of *Psa*.

References

Abada E M, Balzer A, Jager A, Klug G. 2002. Bacteriochlorophyll-dependent expression of genes for pigment-binding proteins in *Rhodobacter capsulatus* involves the RegB/RegA two-component system. *Molecular Genetics and Genomics,* **267**, 202-209.

Anderson J C, Wan Y, Kim Y M, Pasa-Tolic L, Metz T O, Peck S C. 2014. Decreased abundance of type III secretion system-inducing signals in Arabidopsis mkp1 enhances resistance against *Pseudomonas syringae*. *Proceedings of the National Academy of Sciences of the United States of America,* **111**, 6846-6851.

Butler M I, Stockwell P A, Black M A, Day R C, Lamont I L, Poulter R T. 2013. *Pseudomonas syringae* pv. *actinidiae* from recent outbreaks of kiwifruit bacterial canker belong to different clones that originated in China. *PLoS One,* **8**, e57464.

Cao Z, Buttani V, Losi A, Gartner W. 2008. A blue light inducible two-component signal transduction system in the plant pathogen *Pseudomonas syringae* pv. *tomato*. *Biophysical Journal,* **94**, 897-905.

Donati I, Cellini A, Sangiorgio D, Vanneste J L, Scortichini M, Balestra G M, Spinelli F. 2020. *Pseudomonas syringae* pv. *actinidiae*: Ecology, Infection Dynamics and Disease Epidemiology. *Microbial Ecology,* **80**, 81-102.

Duan K, Dammel C, Stein J, Rabin H, Surette M G. 2003. Modulation of *Pseudomonas aeruginosa* gene expression by host microflora through interspecies communication. *Molecular Microbiology,* **50**,

1477-1491.

Dubbs J M, Bird T H, Bauer C E, Tabita F R. 2000. Interaction of CbbR and RegA* transcription regulators with the *Rhodobacter sphaeroides cbbI* Promoter-operator region. *Journal of Biological Chemistry,* **275**, 19224-19230.

Elsen S, Swem L R, Swem D L, Bauer C E. 2004. RegB/RegA, a highly conserved redox-responding global two-component regulatory system. *Mircobiology and Molecular Biology Reviews,* **68**, 263-279.

Fishman M R, Zhang J, Bronstein P A, Stodghill P, Filiatrault M J. 2018. Ca(2+)-Induced Two-Component System CvsSR Regulates the Type III Secretion System and the Extracytoplasmic Function Sigma Factor AlgU in *Pseudomonas syringae* pv. *tomato* DC3000. *Journal of Bacteriology,* **200**. e00538-17.

Fujikawa T, Sawada H. 2019. Genome analysis of *Pseudomonas syringae* pv. *actinidiae* biovar 6, which produces the phytotoxins, phaseolotoxin and coronatine. *Scientific Reports,* **9**, 3836.

Giacomini A, Corich V, Ollero F J, Squartini A, Nuti M P. 1992. Experimental conditions may affect reproducibility of the beta-galactosidase assay. *FEMS Microbiology Letters,* **100**, 87-90.

Kanehisa M, Araki M, Goto S, Hattori M, Hirakawa M, Itoh M, Katayama T, Kawashima S, Okuda S, Tokimatsu T, Yamanishi Y. 2008. KEGG for linking genomes to life and the environment. *Nucleic Acids Research,* **36**, D480-484.

Karimova G, Pidoux J, Ullmann A, Ladant D. 1998. A bacterial two-hybrid system based on a reconstituted signal transduction pathway. *Proceedings of the National Academy of Sciences of the United States of America,* **95**, 5752-5756.

Kim G H, Jung J S, Koh Y J. 2017. Occurrence and Epidemics of Bacterial Canker of Kiwifruit in Korea. *Journal of Plant Pathology,* **33**, 351-361.

Kruger N J. 1994. The Bradford method for protein quantitation. *Methods in Molecular Biology,* **32**, 9-15.

Kvitko B H, Collmer A. 2011. Construction of *Pseudomonas syringae* pv. *tomato* DC3000 mutant and polymutant strains. *Methods in Molecular Biology,* **712**, 109-128.

Li H, Durbin R. 2010. Fast and accurate long-read alignment with Burrows-Wheeler transform. *Bioinformatics,* **26**, 589-595.

Maarsingh J D, Yang S, Park J G, Haydel S E. 2019. Correction to: Comparative transcriptomics reveals PrrABmediated control of metabolic, respiration, energy-generating, and dormancy pathways in *Mycobacterium smegmatis*. *BMC Genomics,* **21**, 1.

Moriconi V, Sellaro R, Ayub N, Soto G, Rugnone M, Shah R, Pathak G P, Gartner W, Casal J J. 2013. LOV-domain photoreceptor, encoded in a genomic island, attenuates the virulence of *Pseudomonas syringae* in light-exposed Arabidopsis leaves. *The Plant Journal,* **76**, 322-331.

Mosley C S, Suzuki J Y, Bauer C E. 1994. Identification and molecular genetic characterization of a sensor kinase responsible for coordinately regulating light harvesting and reaction center gene expression in response to anaerobiosis. *Journal of Bacteriology,* **176**, 7566-7573.

O'Malley M R, Chien C F, Peck S C, Lin N C, Anderson J C. 2020. A revised model for the role of GacS/GacA in regulating type III secretion by *Pseudomonas syringae* pv. *tomato* DC3000. *Molecular Plant Pathology,* **21**, 139-144.

O'Malley M R, Weisberg A J, Chang J H, Anderson J C. 2019. Re-evaluation of a Tn5::gacA mutant of *Pseudomonas syringae* pv. *tomato* DC3000 uncovers roles for uvrC and anmK in promoting virulence. *PLoS One,* **14**, e0223637.

Phenn J, Pane-Farre J, Meukow N, Klein A, Troitzsch A, Tan P, Fuchs S, Wagner G E, Lichtenegger S, Steinmetz I, Kohler C. 2021. RegAB Homolog of *Burkholderia pseudomallei* is the Master Regulator of Redox Control and involved in Virulence. *PLoS Pathogens,* **17**, e1009604.

Sganga M W, Bauer C E. 1992. Regulatory factors controlling photosynthetic reaction center and light-harvesting

gene expression in *Rhodobacter capsulatus*. *Cell,* **68**, 945-954.

Shen H, Keen N T. 1993. Characterization of the promoter of avirulence gene D from *Pseudomonas syringae* pv. *tomato*. *Journal of Bacteriology,* **175**, 5916-5924.

Song Y, Xiao X, Li C, Wang T, Zhao R, Zhang W, Zhang L, Wang Y, Shen X. 2015. The dual transcriptional regulator RovM regulates the expression of AR3- and T6SS4-dependent acid survival systems in response to nutritional status in *Yersinia pseudotuberculosis*. *Environmental Microbiology,* **17**, 4631-4645.

Stonehouse W, Gammon C S, Beck K L, Conlon C A, von Hurst P R, Kruger R. 2013. Kiwifruit: our daily prescription for health. *Canadian Journal of Physiology and Pharmacology,* **91**, 442-447.

Su Z, Chen H, Wang P, Tombosa S, Du L, Han Y, Shen Y, Qian G, Liu F. 2017. 4-Hydroxybenzoic acid is a diffusible factor that connects metabolic shikimate pathway to the biosynthesis of a unique antifungal metabolite in *Lysobacter enzymogenes*. *Molecular Microbiology,* **104**, 163-178.

Swem L R, Elsen S, Bird T H, Swem D L, Koch H G, Myllykallio H, Daldal F, Bauer C E. 2001. The RegB/RegA two-component regulatory system controls synthesis of photosynthesis and respiratory electron transfer components in *Rhodobacter capsulatus*. *Journal of Molecular Biology,* **309**, 121-138.

Vanneste J L, Cornish D A, Yu J, Stokes C A. 2014. First Report of *Pseudomonas syringae* pv. *actinidiae* the Causal Agent of Bacterial Canker of Kiwifruit on Actinidia arguta Vines in New Zealand. *Plant Disease,* **98**, 418.

Wang T, Chen K, Gao F, Kang Y, Chaudhry M T, Wang Z, Wang Y, Shen X. 2017. ZntR positively regulates T6SS4 expression in *Yersinia pseudotuberculosis*. *Journal of Microbiology,* **55**, 448-456.

Xiao Y, Hutcheson S W. 1994. A single promoter sequence recognized by a newly identified alternate sigma factor directs expression of pathogenicity and host range determinants in *Pseudomonas syringae*. *Journal of Bacteriology,* **176**, 3089-3091.

Xiao Y, Lu Y, Heu S, Hutcheson S W. 1992. Organization and environmental regulation of the *Pseudomonas syringae* pv. *syringae* 61 *hrp* cluster. *Journal of Bacteriology,* **174**, 1734-1741.

Xie Y, Shao X, Deng X. 2019a. Regulation of type III secretion system in *Pseudomonas syringae*. *Environmental Microbiology l,* **21**, 4465-4477.

Xie Y, Shao X, Zhang Y, Liu J, Wang T, Zhang W, Hua C, Deng X. 2019b. *Pseudomonas savastanoi* Two-Component System RhpRS Switches between Virulence and Metabolism by Tuning Phosphorylation State and Sensing Nutritional Conditions. *Microbial Biotechnology,* **10**, e02838-18.

Yan Q, Rogan C J, Pang Y Y, Davis E W, 2nd, Anderson J C. 2020. Ancient co-option of an amino acid ABC transporter locus in *Pseudomonas syringae* for host signal-dependent virulence gene regulation. *PLoS Pathogens,* **16**, e1008680.

Yang S, Peng Q, San Francisco M, Wang Y, Zeng Q, Yang C H. 2008. Type III secretion system genes of *Dickeya dadantii* 3937 are induced by plant phenolic acids. *PLoS One,* **3**, e2973.

Zhang L, Dong T, Yang J, Hao S, Sun Z, Peng Y. 2023. Anammox Coupled with Photocatalyst for Enhanced Nitrogen Removal and the Activated Aerobic Respiration of Anammox Bacteria Based on cbb3-Type Cytochrome c Oxidase. *Environmental Science & Technology,* **57**, 17910-17919.

Zhao F, Zhi T, Hu R, Fan R, Long Y, Tian F, Zhao Z. 2022. The OmpR-like Transcription Factor as a Negative Regulator of hrpR/S in *Pseudomonas syringae* pv. *actinidiae*. *International Journal of Molecular Sciences,* **23**,12036.

Zhao Z, Chen J, Gao X, Zhang D, Zhang J, Wen J, Qin H, Guo M, Huang L. 2019. Comparative genomics reveal pathogenicity-related loci in *Pseudomonas syringae* pv. *actinidiae* biovar 3. *Molecular Plant Pathology,* **20**, 923-942.